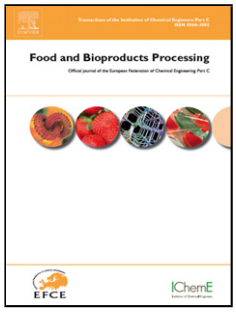

Title: Effect of surface conditioning with cellular extracts on *Escherichia coli* adhesion and initial biofilm formation

Authors: J.M.R. Moreira, L.C. Gomes, K.A. Whitehead, S. Lynch, L.A. Tetlow, F.J. Mergulhão

PII: S0960-3085(17)30041-X
DOI: http://dx.doi.org/doi:10.1016/j.fbp.2017.03.008
Reference: FBP 854

To appear in: *Food and Bioproducts Processing*

Received date: 3-7-2016
Revised date: 25-12-2016
Accepted date: 26-3-2017

Please cite this article as: Moreira, J.M.R., Gomes, L.C., Whitehead, K.A., Lynch, S., Tetlow, L.A., Mergulhão, F.J., Effect of surface conditioning with cellular extracts on Escherichia coli adhesion and initial biofilm formation.Food and Bioproducts Processing http://dx.doi.org/10.1016/j.fbp.2017.03.008

Effect of surface conditioning with cellular extracts on *Escherichia coli* adhesion and initial biofilm formation

Moreira J.M.R.[a], Gomes L.C.[a], Whitehead K.A.[b], Lynch S.[c], Tetlow L.A.[b] and Mergulhão F.J.[a]*

a - LEPABE - Department of Chemical Engineering, Faculty of Engineering, University of Porto, Portugal

b - School of Healthcare Science, Manchester Metropolitan University, UK

c - School of Computing, Mathematics and Digital Technology, Manchester Metropolitan University, UK

*Corresponding author. Mailing address: Department of Chemical Engineering, Faculty of Engineering University of Porto, Rua Dr. Roberto Frias s/n, 4200-465 Porto, Portugal. Phone: (+351) 225081668. Fax: (+351) 5081449. E-mail: filipem@fe.up.pt.

Graphical abstract

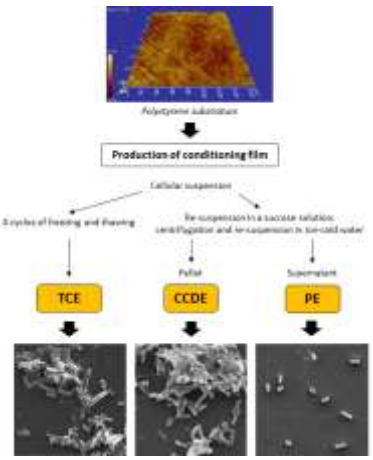

Highlights

- Microplate assays demonstrated that TCE and CCDE decreased initial biofilm formation
- Cell adhesion generally increased when PE was used
- Biofilm formation was dependent on the conditioning film concentration
- Under flow conditions all conditioning films reduced biofilm formation
- Surface conditioning affected the amount and clustering of bacteria on surfaces

Abstract

Bacterial adhesion and subsequent biofilm formation start with surface conditioning by molecules originating from the surrounding medium and from cell lysis. Different cell extracts e.g. total cell extract (TCE), cytoplasm with cellular debris (CCDE) and periplasmic extract (PE) were tested in agitated 96-well microtiter plates and in a flow cell. Crystal violet assay demonstrated that a polystyrene substratum conditioned with TCE or CCDE decreased initial biofilm formation, however cell adhesion generally increased when PE was used. These results were dependent on conditioning film concentration. Using a parallel plate flow chamber, the use of optimal conditioning film concentrations resulted in all the different cellular extracts reducing biofilm formation. Multifractal analysis was used to generate quantitative data on the number of cell clusters. Surface conditioning with cellular components affected the amount and clustering of bacteria on polystyrene surfaces and their propensity to induce biofilm formation. To the best of our knowledge, this is the first study addressing the effect of cellular surface conditioning of cellular compartments on *E. coli* adhesion and initial biofilm formation. This work leads to a greater understanding of the factors that influence biofilm formation under flow conditions which are prevalent in food industry.

Keywords: Adhesion; surface conditioning; periplasm; cytoplasm; multifractal analysis;

biofilms

1. Introduction

The contamination of food contact surfaces by residual organic materials and food-borne microorganisms in the food processing industries has been an ever-persistent issue. Organic material on a surface will affect cell-substratum interactions, and will introduce additional cell-organic material and organic material-substratum interactions (Whitehead and Verran, 2015). Such biofouling may result in increasing or decreasing cell viability and surface cleanability. Retained organic material on a surface may also impede the recovery of cells or may protect cells from cleaning agents (Bernbom et al., 2011; Whitehead et al., 2009b). Bacterial adhesion and subsequent biofilm development start with surface conditioning with molecules originating from the surrounding medium, since these molecules will diffuse faster than bacterial cells due to their reduced size (Bruinsma et al., 2001). The formation of conditioning layers may take from few seconds to some minutes (Garrido et al., 2014). Following surface conditioning, bacteria will become attached, adhered and then retained on a surface (Whitehead and Verran, 2015). It is at this point that proliferation of the bacteria may result in biofilm formation. Since the nature of the initial surface chemistry will influence bacterial attachment and retention, it may be speculated that the type of conditioning film present will in turn affect biofilm formation (Whitehead and Verran, 2015).

Biofilms are microbial communities attached to surfaces and surrounded by a matrix of extracellular polymeric substances (EPS). Conditioning agents may be components of the culture medium or cell-derived components originating from cell lysis such as individual molecules or cellular debris fragments (Renner and Weibel, 2011). A wide variety of polymers can be found in the biofilm matrix, but the major components are proteins and polysaccharides, whereas lipids and nucleic acids are found in minor quantities (Ras et al.,

2011). These compounds are excreted by the microbial population, but can also result from natural cell lysis and from hydrolytic or cleaning activities (Ras et al., 2011). Although cell adhesion is usually affected by the properties of the original unconditioned surface, it can also be altered by the formation of a conditioning film (Hwang et al., 2012; Hwang et al., 2013). The effects of conditioning films on bacterial adhesion have been widely discussed in the literature with contradictory findings, probably due to the diversity of environmental conditions that the surfaces were exposed to (Hwang et al., 2013; Lorite et al., 2011). For instance, it was demonstrated that the presence of alginate and other organic matter in conditioning films significantly increased initial bacterial adhesion onto glass surfaces at low ionic strength, nonetheless adhesion was not enhanced by bovine serum albumin (BSA) conditioning (Hwang et al., 2012). Recently, Ribeiro et al. (2017) observed higher adhesion of *Bacillus cereus* spores when using whole milk as conditioning matrix compared to the unconditioned stainless steel surface (4.93 versus 3.01 log CFU cm^{-2}), suggesting an interaction between milk fat and bacteria on the surface. In opposition, it has also been shown that preconditioning of stainless steel with aqueous cod muscle extract significantly impeded bacterial adhesion (Bernbom et al., 2009). Hamadi et al. (2014) studied the adhesion of *Staphylococcus aureus* to stainless steel treated with three types of milk and found that they reduced bacterial attachment. Moreover, the lowest and the highest adhesion values were obtained when the surface was treated by the semi-skimmed milk and skimmed milk, respectively, showing that adhesion is affected by fat content (Hamadi et al., 2014). Recently, it was found that adsorption of alginate and albumin onto aluminum coatings inhibited *Escherichia coli* adhesion by altering the surface hydrophobicity (He et al., 2015). This conditioning layer also enhanced the anti-corrosion performance of the coatings (He et al., 2015). Additionally, other authors have shown that protein films reduced the bacterial adhesion to different surfaces (Chapman et al., 2001; Dat et al., 2014; Merghni et al., 2016;

Robitaille et al., 2014).

Quantification of the percentage coverage of retained cells in a monolayer following epifluorescence microscopy has been carried out for some time (Whitehead and Verran, 2007). However, the development of a quantifiable method to determine the percentage coverage of both conditioning film and cells on a surface has proved to be more difficult, but can be achieved using certain staining methods (Whitehead et al., 2009b). Multifractal analysis has been used to obtain numerical data on the effect of surface properties on cell dispersion, density and clustering (Wickens et al., 2014). In this work, multifractal analysis has been used in order to demonstrate the level of cell/biofilm clustering and overall percentage coverage of the bacteria and biofilms on the surfaces following conditioning with cellular extracts. Understanding, comparing and quantifying how the patterns of cellular adhesion and biofilm formation occur across a surface is imperative for designing hygienic surfaces in the future.

Despite the investigation of surface conditioning effects on cell adhesion, there are few studies analysing the impact of cellular surface conditioning components on biofilm formation. Further, this work used the determination of the upper bacterial/biofilm percentage coverage to quantify the number of clusters present. The present study evaluates the effect of cellular components as surface conditioning agents and quantifies their impact on initial biofilm formation under flow conditions.

2. Material and Methods

2.1. Bacteria and culture conditions

E. coli JM109(DE3) from Promega (USA) was used in this study because it has shown a good biofilm forming capacity in a diversity of platforms operated at different shear stresses (Gomes et al., 2014; Moreira et al., 2015b; Teodósio et al., 2011). Additionally, it was shown

that its biofilm formation was similar to other *E. coli* strains which are often used for antimicrobial susceptibility tests (Gomes et al., 2014). The strain was grown overnight at 30ºC and 120 rpm after the inoculation of 500 µl of a glycerol stock kept at -80ºC in 0.2 l of culture medium (Teodósio et al., 2011). This medium consisted of 5.5 g l^{-1} glucose, 2.5 g l^{-1} peptone, 1.25 g l^{-1} yeast extract in phosphate buffer (1.88 g l^{-1} KH_2PO_4 and 2.60 g l^{-1} Na_2HPO_4), pH 7.0. All medium components were purchased from Merck KGaA (Germany). Cells were then centrifuged (3202 *g*, 10 min) and washed twice with citrate buffer 0.05 mol l^{-1}, pH 5.0 (Moreira et al., 2015b). The pellet was resuspended in citrate buffer and the cellular suspension was adjusted to a final concentration of 7.6×10^7 cell ml^{-1} determined by optical density at 610 nm ($OD_{610\ nm}$ = 0.1). This cell suspension was used for initial biofilm formation assays in 96-well microtiter plates and in a parallel plate flow chamber (PPFC).

2.2 Conditioning agents

Three different types of cellular extracts were tested as conditioning agents: total cell extract (TCE), cytoplasm with cellular debris (CCDE) and periplasmic extract (PE). Cells from an overnight culture were harvested by centrifugation and washed twice with distilled water. The pellet was concentrated and re-suspended in water to reach a cell concentration of 30.4×10^8 cell ml^{-1} ($OD_{610\ nm}$ = 4.0). This cell suspension was then divided in two parts, one part for the preparation of PE and CCDE, and another to prepare the TCE. The TCE was obtained by subjecting this cellular suspension ($OD_{610\ nm}$ = 4.0) to four cycles of freezing (at - 80ºC) and thawing (in a water bath at 30ºC). To prepare the PE (Mergulhão et al., 2001), the initial suspension ($OD_{610\ nm}$ = 4.0) was centrifuged again, re-suspended in a sucrose solution (20% sucrose, 0.3 mol l^{-1} Tris-HCl pH 8.0, 1 mmol l^{-1} EDTA) and incubated at room temperature for 15 min. This suspension was centrifuged (6000 *g*, 10 min), and the pellet was re-suspended in ice-cold water and incubated for 15 min on ice. This mixture was centrifuged

(12000 *g*, 10 min) and the PE was obtained in the supernatant, whereas the pellet was re-suspended in ice-cold water and the cells were disrupted by sonication (Sonopuls HD 2070, Bandelin Electronics, Germany) (7 cycles of 30 s at 20 Hz) yielding the CCDE. The TCE, CCDE and PE that were obtained from a cell suspension with an $OD_{610\ nm}$ = 4.0 were further diluted in water to recreate cell suspensions with cellular concentrations of (0.38, 0.76, 3.04, 6.08, 12.2 and 24.3) × 10^8 cell ml^{-1}.

2.3 96-well microtiter plate assay

Six wells of sterile 96-well polystyrene, flat-bottomed microtiter plates (Orange Scientific, USA) were filled with 200 µl of the conditioning agent at each desired concentration. The plates were incubated for 1 h at 30ºC with agitation (50 mm of orbital shaking diameter at 150 rpm) in order to obtain a shear stress of 0.07 Pa as determined by computational fluid dynamics (not shown). After surface conditioning, each well was washed (Martinez and Casadevall, 2007; Pratt-Terpstra et al., 1987) with 200 µl of citrate buffer 0.05 mol l^{-1}, pH 5.0, and filled with 200 µl of cell suspension (7.6 × 10^7 cell ml^{-1} in citrate buffer). To promote bacterial adhesion and initial biofilm formation, the plates were again incubated at 30ºC with agitation for 24 h. Unconditioned surfaces were used as control. Three independent experiments were made.

Biofilm quantification using a crystal violet assay was performed (Moreira et al., 2013). The content of the microtiter plates was discarded and the wells were washed with sterile water to remove non-adherent cells. Retained cells were fixed with 250 µl of 96% ethanol for 15 min and stained for 5 min with 200 µl of 1% (v/v) crystal violet (Merck KGaA, Germany) per well. The plates were again emptied and the bound dye was solubilized with 200 µl of 33% (v/v) acetic acid (VWR, Portugal) per well. The OD was measured at 570 nm using a microtiter plate reader (SpectraMax M2E, Molecular Devices, UK) and the number of cells

retained/initial biofilm amount was expressed as $OD_{570\ nm}$ values.

2.4 Parallel plate flow chamber assay

The most effective concentrations of the conditioning agents determined in the 96-well microtiter plate assay were further tested in a PPFC in order to allow biofilm staining and scanning electron microscopy (SEM) analysis. TCE and CCDE were used at a concentration corresponding to 24.3×10^8 cell ml^{-1}, while PE was tested at 0.38×10^8 cell ml^{-1}.

The PPFC was coupled to a tank and to a centrifugal pump by a tubing system to conduct the assay (Moreira et al., 2014). The PPFC contained recesses in the bottom for the introduction of polystyrene coupons (1 cm diameter) in order to obtain a flush surface in contact with the bacterial suspension circulating in the system. Polystyrene is one of the most commonly plastic used in the food industry, mainly for packaging (Di Ciccio et al., 2015; Mahalik and Nambiar, 2010). Before being introduced into the PPFC, the polystyrene coupons were washed for 5 min with a commercial detergent (Sonasol Pril; Henkel Ibérica, S.A., Spain), immersed in sodium hypochlorite (3%) and finally washed with distilled water.

The PPFC was first conditioned for 1 h at the same average shear stress operated in the microtiter plates (0.07 Pa), which corresponded to a flow rate of 11 ml s^{-1} (Moreira et al., 2014). Then, a washing step with citrate buffer was performed and the *E. coli* suspension with an $OD_{610\ nm}$ = 0.1 was circulated through the PPFC at a flow rate of 11 ml s^{-1}. The temperature of the flow cell system was kept constant at 30ºC using a recirculating water bath. Unconditioned polystyrene coupons were used as control. After 24 h, coupons were removed from the PPFC and total bacterial counts were obtained by direct staining with 4',6-diamidino-2-phenylindole (DAPI) (Moreira et al., 2015a). Cells were visualized under an epifluorescence microscope (Eclipse LV100; Nikon, Japan) equipped with a filter block sensitive to DAPI fluorescence (359-nm excitation filter in combination with a 461-nm

emission filter). For each coupon, a minimum of 10 fields were counted and the results were expressed as number of retained cells per cm^2. Three independent experiments were performed for each conditioning agent and for unconditioned coupons.

Coupons were also prepared for SEM analysis and all samples were fixed and dehydrated as previously described (Gomes et al., 2013). Coupons were air-dried for 1 day in a desiccator and sputter-coated with a palladium-gold thin film (Gomes et al., 2013) using a SPI Module Sputter Coater equipment for 70 s at 15 mA current. Samples were analysed using a SEM/EDS system (FEI Quanta 400FEG ESEM/EDAX Genesis X4M; FEI Company, USA) operated in high-vacuum mode at 15 kV. Twenty images from the bare surface, the unconditioned surface, the substrata with conditioning films and the 24 h retained cells/initial biofilms formed on the conditioned surfaces were analysed (three different coupons for each tested condition were used).

2.5 Multifractal analysis

This analysis is a further development of the method previously described in Wickens et al. (2014). To illustrate the properties of typical multifractal spectra, multifractal datasets were constructed from a set of motifs using MATLAB®. Using a simple iterative program, matrix (datasets) of size 512 × 512 were computed by overlaying the given motifs one on top of another, so that upon the first iteration a 4 × 4 matrix was formed, upon the second iteration an 8 × 8 matrix was formed, until completion. Using the MathWorks Image Processing Toolbox®, the datasets were converted into grey scale images whereby a value of zero would give black on this scale and a value of one would give white. The numerical $f(\alpha)$ spectra were computed for, $-10 \leq q \leq 10$, and boxes of size $\varepsilon = 4$, 8, 16, 32, 64, 128 and 256, were used to fully cover the datasets. From the $f(\alpha)$ curves there are values that can be extrapolated which denote the numerical values of the cell density, clustering and dispersion.

As this paper is concerned with clustering and biofilm formation only, only the symmetry of the $f(\alpha)$ curves was considered. This technique can also be used to determine density and dispersion (Mills et al., 2004; Mills et al., 2005; Wickens et al., 2014). The quantity $\Delta\alpha_{AS} = \alpha_{max} - \alpha_{min}$ describes the heterogeneity of the cell spread on the surface and can be used to measure clustering (Wickens et al., 2014).

Multifractal analysis has been applied to provide statistical properties for the objects in terms of their generalised (box-counting) fractal dimensions (Hentschel and Procaccia, 1983) or their singularity spectra (Halsey et al., 1986). The generalised (box-counting) fractal dimensions, D_q, where $q \in R$ (where q is a real number), are defined by:

$$D_q = \lim_{\varepsilon \to 0} \frac{1}{1-q} \frac{ln\left(\sum_{i=1}^{N} p_i^q(\varepsilon)\right)}{-ln(\varepsilon)} \qquad (1)$$

where the index i labels individual boxes of size ε and $p_i(\varepsilon)$ represents the relative weight of the i'th box or the probability of the object lying in the box. In applications, the so-called $f(\alpha)$ spectra are usually applied, which are an alternate form for the D_q spectra. Using the methods outlined in Lynch (2014), the $f(\alpha)$ spectra are computed as follows:

$$f(q) = \lim_{\varepsilon \to 0} \frac{\sum_{i=1}^{N} \mu_i(q,\varepsilon) ln\left(\mu_i(q,\varepsilon)\right)}{ln(\varepsilon)} \qquad (2)$$

and

$$\alpha(q) = \lim_{\varepsilon \to 0} \frac{\sum_{i=1}^{N} \mu_i(q,\varepsilon) ln\left(p_i(\varepsilon)\right)}{ln(\varepsilon)} \qquad (3)$$

where

$$\mu_i(q,\varepsilon) = \frac{p_i^q(\varepsilon)}{\sum_{j=1}^{N} p_j^q(\varepsilon)} \qquad (4)$$

The exponents α_S and f_S were then used to determine the $f(\alpha)$ spectrum. In many cases,

$f(\alpha)$ is related to the Hausdorff-Besicovich dimension (Falconer, 2013, 2014). The image to be analysed was covered with boxes of size ε and the corresponding box-measures $\mu_i(\varepsilon) = p_i(\varepsilon)$ were computed. A typical $f(\alpha)$ curve was plotted where D_0 represents the fractal dimension (this gives a measure of density) (Fig. 1). The minimum value of α was denoted by "α_{min}" ($q = +\infty$). The "α_{max}" was the point at which the curve intersected with the x-axis at $q = -\infty$. The "α_0" depicts the value at which the maximum of $f(\alpha)$ exists. Using the data cursor in MATLAB®, the two points α_{max} and α_{min} were estimated and used to give a measure of the dispersion (Δ_∞) as follows:

$$\Delta_\infty = \alpha_{max} - \alpha_{min} \qquad (5)$$

A measure of asymmetry ($\Delta\alpha_{AS}$) is given by:

$$\Delta\alpha_{AS} = \frac{\alpha_0 - \alpha_{min}}{\alpha_{max} - \alpha_0} \qquad (6)$$

The $f(\alpha)$ curve is symmetric if $\Delta\alpha_{AS} = 1$, left-skewed if $\Delta\alpha_{AS} > 1$, and right-skewed if $\Delta\alpha_{AS} < 1$.

Motifs of multifractal objects along with their images and $f(\alpha)$ spectra are demonstrated in Fig. 2. A left-skewed $f(\alpha)$ curve depicts clusters of gaps and a right-skewed $f(\alpha)$ curve depicts clustering of bright pixels, or cells and biofilm, in this case.

2.6 Surface characterization

Surface hydrophobicity was evaluated considering the Lifshitz-van der Waals acid base approach (van Oss, 1994). The contact angles were determined automatically by the sessile

drop method in a contact angle meter (OCA 15 Plus; Dataphysics, Germany) using water, formamide and α-bromonaphtalene (Sigma-Aldrich Co., Portugal) as reference liquids (Janczuk et al., 1993). The surface tension components of the reference liquids were taken from literature (Janczuk et al., 1993). For each surface, measurements with each liquid were performed at 25 ± 2ºC. The model proposed by van Oss (1994) indicates that the total surface energy (γ^{Tot}) of a pure substance is the sum of the Lifshitz-van der Waals components of the surface free energy (γ^{LW}) and Lewis acid-base components (γ^{AB}):

$$\gamma^{Tot} = \gamma^{LW} + \gamma^{AB} \qquad (7)$$

The polar AB component comprises the electron acceptor (γ^{+}) and electron donor (γ^{-}) parameters, and is given by:

$$\gamma^{AB} = 2\sqrt{\gamma^{+} + \gamma^{-}} \qquad (8)$$

The surface energy components of a solid surface (s) are obtained by measuring the contact angles (θ) with the three different liquids (l) with known surface tension components, followed by the simultaneous resolution of three equations of the type:

$$(1 + \cos\theta)\gamma_l{}^{Tot} = 2\left(\sqrt{\gamma_s^{LW}\gamma_l^{LW}} + \sqrt{\gamma_s^{+}\gamma_l^{-}} + \sqrt{\gamma_s^{-}\gamma_l^{+}}\right) \qquad (9)$$

The degree of hydrophobicity of a given surface is expressed as the free energy of interaction (ΔG) between two entities of that surface immersed in a polar liquid (such as water (w) as a model solvent). ΔG was calculated from the surface tension components of the interacting entities, using the equation:

$$\Delta G = -2\left(\sqrt{\gamma_s^{LW}} - \sqrt{\gamma_w^{LW}}\right)^2 + 4\left(\sqrt{\gamma_s^{+}\gamma_w^{-}} + \sqrt{\gamma_s^{-}\gamma_w^{+}} - \sqrt{\gamma_s^{+}\gamma_s^{-}} - \sqrt{\gamma_w^{+}\gamma_w^{-}}\right) \qquad (10)$$

If the interaction between the two entities is stronger than the interaction of each entity with

water, ΔG < 0 mJ m^{-2}, the material is considered hydrophobic; if ΔG > 0 mJ m^{-2}, the material is hydrophilic.

The topography of the surfaces was measured using white light profilometry. Surface roughness was defined quantitatively through measurement of S_a, S_q and S_{pv} values using a Zemetrics, Zegage 3D optical profiler (Zygo, USA) with AD phase shift controller (Ominscan, UK). The S_a represents the average surface roughness of the profile height deviations whilst S_q is the root mean square of the defined surface roughness. S_{pv} describes the value of the peak to valley surface roughness. Five areas of five replicates (n = 25) were analysed at 50× magnification. The image analysis software used was Zemaps (version 1.14.38).

Surface analysis by contact angle measurement and light profilometry was performed on the non-conditioned polystyrene surface and also on the conditioned surfaces using the same extract concentrations of the PPFC assay (TCE and CCDE were used at a concentration corresponding to 24.3 × 10^8 cell ml^{-1}, while PE was tested at 0.38 × 10^8 cell ml^{-1}).

3. Results and Discussion

The impact of surface conditioning on *E. coli* initial biofilm formation was evaluated using either a microtiter plate crystal violet assay or a PPFC, following which the surfaces were analysed by DAPI (quantitative) or SEM (qualitative). Multifractal analysis was then used to generate binary images, f (α) curves and histograms in order to determine the percentage coverage of the bacteria/upper biofilm on the surfaces and thus calculate the number of cell clusters present.

In a first step, the physicochemical characterization of the polystyrene surface before and after conditioning was made by contact angle measurement (Table 1). From the total free energy results it was possible to observe that the polystyrene surface was initially

hydrophobic (ΔG < 0 mJ m^{-2}). When the polystyrene surface was conditioned with the conditioning agents at the concentration with the greatest impact on initial biofilm formation (conditions used in the PPFC assay), the surface hydrophobicity remained almost the same for PE and was significantly reduced for TCE and CCDE. Previous work on the effect of conditioning films on the physicochemical properties of surfaces demonstrated that the addition of organic material resulted in changes to the substratum physicochemistries at the surface/bacterial interface (Whitehead et al., 2009a).

The bare polystyrene surface was imaged (Fig. 3) and analysed in terms of surface roughness using the parameters, (S_a, S_q and S_{pv}) (Table 1). The results demonstrated that overall, the polystyrene had low roughness values (S_a average 8.01 nm). The S_q values were marginally greater (12.1 nm), whilst as expected the S_{pv} values demonstrated the greatest differences (1082 nm). This is due to some surface features that became evident during imaging, however these were not periodic or regular in form across the surfaces. An advantage of using S_q measurements alongside S_a measurements is that that a single large peak or flaw within the surface roughness will increase the S_q value more than the S_a value, and this was precisely what was demonstrated (Whitehead and Verran, 2006). The line profile demonstrated that the surface features were in the order of nanoscale dimensions (< 0.5 µm) in terms of both width and height.

After conditioning with PE, the surface roughness was not affected, but conditioning with TCE and CCDE increased the average surface roughness (S_a) (Table 1). Since a similar

number of adhered cells was detected after a 24 h period on all conditioned surfaces (Fig. 5), it was possible to conclude that the reduction in biofilm formation upon conditioning was not caused by the change in surface roughness.

A PPFC and a 96-well microtiter plate assay under agitation were used to determine the effect of cellular extracts on biofilm formation in flow systems. Screening of TCE, PE and cytoplasm with cellular debris (CCDE) in different concentrations was conducted in agitated 96-well microtiter plates (Fig. 4) to take advantage of the high-throughput of this platform. Since flow systems are typical of industrial and medical settings, the effect of the most relevant concentrations on bacterial adhesion and initial biofilm development was also tested in a PPFC (Fig. 5). With the aim of maintaining similar operational conditions in both platforms, the same surfaces (bare and conditioned polystyrene) were used and the PPFC was operated at a flow rate that yielded the same average wall shear stress than the one obtained in the 96-well microtiter plate (0.07 Pa).

All tested extracts in all concentrations caused a reduction in biofilm formation using the crystal violet assay (Fig. 4) when compared to the unconditioned surface ($P < 0.05$), except for the highest concentration of PE where the difference was not statistically significant. For TCE and CCDE conditioned surfaces, higher biofilm reductions were obtained at higher concentrations of conditioning agent (Fig. 4a and b) with an average reduction of 60%. PE showed a different behavior from the other conditioning agents (Fig. 4c) as the lowest tested concentration resulted in the greatest reduction.

For each cell extract, the concentration with the greatest impact on initial biofilm formation in the microtiter plate assay was tested in the PPFC (Fig. 5). Results showed that initial biofilm formation under flow was reduced by all the conditioning films tested (by about 60%), which agreed with the results obtained in the microtiter plate assays. In agreement with

our work, *S. aureus* adhesion forces have been demonstrated to decrease in the presence of salivary conditioning films on various dental restorative materials (Merghni et al., 2016).

Contact angle analysis has shown that polystyrene hydrophobicity changed upon surface conditioning and that hydrophobicity was significantly reduced upon conditioning with TCE and CCDE (Table 1). Since a similar amount of adhered cells was detected between the conditioned surfaces (Fig. 5), the decrease in biofilm formation upon conditioning (relative to the control) was not related with the variation on surface hydrophobicity. Surface roughness was affected after conditioning with TCE and CCDE (Table 1) and therefore it is possible to conclude that the decrease in biofilm formation was also not due to a change in surface roughness. Hwang et al. (Hwang et al., 2012; Hwang et al., 2013) coated slides with model EPS components and determined that the surface roughness in the presence of conditioning film on initial bacterial adhesion was not significant. Further, they concluded that forces other than hydrophobic and electrostatic interactions were involved in controlling bacterial adhesion to BSA-coated surfaces (Hwang et al., 2012; Hwang et al., 2013). Therefore, along with our work, the authors suggest that the differences observed in cell retention were not a result of the changes in the surface chemistry due to the presence of conditioning films.

SEM showed that the morphology of the different conditioning films once applied to the surface varied greatly (Fig. 6c, e and g). Surface conditioning was clearly observed for TCE and CCDE where the presence of cellular debris in localized regions of the coupons could be seen (Fig. 6c and e). However, when TCE was used (Fig. 6c), the cells looked rounded, longer (~ 1 µm x 3 µm) and less damaged. When the CCDE conditioning film was used (Fig. 6e), EPS, organic material and a range of smaller, less rounded looking cells (~ 1 µm x 2 µm)

were distributed more heterogeneously across the surface. Following surface conditioning with PE (Fig. 6g), cell debris and EPS were not evident and gave a similar image to that of the bare substrata. These results demonstrate that although the conditioning extracts were produced from the same source, their components and consequently their differences in biochemistry resulted in a range of cellular and organic material distributions across the surfaces. The uneven distribution of different conditioning films across surfaces has also been demonstrated in a previous work (Whitehead et al., 2010).

The retention of the cellular extracts was also found to affect biofilm development (Fig. 6d, f and h). After 24 h on an unconditioned polystyrene surface, a uniform cell distribution was observed and cells formed a monolayer where EPS could not be visualized (Fig. 6b). Biofilms formed on conditioned surfaces with TCE and CCDE were organized into clusters formed on top of the cellular debris and representative images of those structures can be observed (Fig. 6d and f). When TCE was used as a conditioning agent (Fig. 6d), cells and EPS were clearly evident. The use of CCDE as a conditioning film (Fig. 6f) resulted in large amounts of EPS and organic material as well as dense clusters of well-developed cells (~ 1 µm x 3 µm). The results suggest that when using either TCE or CCDE the initiation of biofilm formation was well established within 24 h. When PE was used for conditioning (Fig. 6h), only a few, small cells (~ 1 µm x 1 µm -2 µm) were evident with little or no EPS production. It is therefore likely that some periplasmic component, when adsorbed to a surface, inhibits EPS production in *E. coli* and delays biofilm formation. SEM visualization of conditioned surfaces and retained cells demonstrated that surface conditioning was not uniform. It is highly probable that biofilm formation started in areas containing cell debris (for both TCE and CCDE) since it is possible that cellular debris may have provided a physical anchoring point for planktonic cells flowing in the surrounding fluid. Nevertheless, an important point is that the adsorbed components had a negative influence on bacterial

adhesion and initial biofilm development; this phenomenon needs to be further investigated. For the PE, it is likely that no significant cell lysis occurred during the extract preparation as no cell debris was detected at the surface. The *E. coli* periplasm contains many different proteins including binding proteins, scavenging enzymes and detoxifying enzymes (Oliver, 1987; Parry et al., 2014). In agreement with our findings, it has been previously reported that surface conditioning with some proteins (e.g. BSA) may decrease initial cell adhesion and biofilm formation (Hammond et al., 2010; Pratt-Terpstra et al., 1987). However, work by Whitehead et al. (2010) demonstrated that different conditioning films result in different patterns of organic material across surfaces (Whitehead et al., 2010). If the findings from Whitehead et al. (2010) are taken in tandem with the results presented here, it may be hypothesized that the pattern and distribution of the underlying conditioning film may affect initial cell adhesion, spatial distribution and subsequent biofilm formation. Stainless steel with an aqueous cod extract was demonstrated to significantly decrease bacterial attachment by a factor of 10-100 (Bernbom et al., 2006) whereas the presence of protein (tryptic soy broth supplemented with horse serum) on food contact surfaces has been shown to significantly increase the number of attaching *Salmonella typhimurium* (Moore et al., 2007). What was not clear from the literature was evidence of work that demonstrated the effect of conditioning films on initial biofilm formation or on the quantification of their distribution in terms of "clusters" across the surfaces.

Multifractal analysis is commonly used to measure density and dispersion of components across a surface and has been used in a number of biological systems (Goldberger et al., 2002; Ivanov et al., 1999; Kropp et al., 1997; Li et al., 2007). In this work, multifractal analysis was used to obtain measurements of the upper percentage coverage of the bacterial cells or biofilm but more importantly, to define a quantitative measurement of the clustering

of cells on the surface. In future work, we hope to be able to correlate this to the underlying surface properties and confocal microscopy images throughout the biofilm in order to determine the factors that enhance initial cell attachment and adhesion.

The $f(\alpha)$ curves from the multifractal analysis demonstrate that if symmetric $f(\alpha)$ curves are obtained then there is no cellular or biofilm clustering. On the other hand, right-skewed $f(\alpha)$ curves indicate clustering of cells and biofilm formation (Fig. 7a) and left-skewed $f(\alpha)$ curves indicate clusters of gaps (e.g. individual cells) (Fig. 7b).

By converting the grey-scale images to binary images and by deleting pixel areas (smaller than a designated value), the cell percentage coverage of the surfaces was calculated. However, when the cells cluster together as it occurs during biofilm formation, it is also important to generate data on the number of clusters. This information was generated by the histograms. A typical histogram (Fig. 8b) demonstrates that there were many cells without much clustering, whereby there is a typical normal distribution at the left hand side of the histogram. In contrast, when the pixel area was much greater (an order of 10), this indicates that the cells were clustered together (Fig. 8f). This data was then quantified to demonstrate the number of clusters in the image.

The results for the percentage coverage (Fig. 9a) were in line with what was observed in the

images (Fig. 6). However, once a biofilm is formed the information of the percentage cell coverage on a surface is not descriptive enough since, although a large area may be covered, the cells may be well distributed or in a single cluster (Whitehead and Verran, 2007). It was demonstrated that the CCDE and the unconditioned surface had the greatest percentage coverage. Work previously carried out using multifractal analysis on the bacterial distribution demonstrated that this method can be used to quantitatively analyse the cell dispersion, density and clustering of retained microorganisms on surfaces (Wickens et al., 2014). However, the authors are unaware of multifractal analysis being used to determine bacterial distribution across a conditioned surface. Multifractal analysis allowed the determination of the cell clustering across the surface (Fig. 9b). When the cells were widely spread out as in the unconditioned surface following 24 h, there was a large percentage coverage and a high number of individual clusters recorded (Fig. 9b). However, when a large amount of biofilm was formed, as it was observed in the conditioned surface following 24 h of incubation, again a large percentage coverage was recorded, but only a small number of clusters was detected (Fig. 9b). Thus, the combination of these two parameters provided further information on the amount of bacterial coverage and the number of clusters. In agreement with Wickens et al. (2014), the results demonstrate that multifractal analysis is a method that can be used to quantitatively analyse the cell clustering of retained microorganisms and biofilms on surfaces, in the presence of a conditioning film. Unfortunately, multifractal analysis does not measure the cells with regards to the depth of the biofilm, but this application is currently being explored. This work will also be further expanded to determine quantitative analysis of live/dead bacteria in biofilms and the distribution of bacteria and conditioning films on surfaces with biofilms.

4. Conclusions

Conditioning of surfaces with cell extracts resulted in different percentage coverages of bacterial adhesion and numbers of cell clustering. Crystal violet assays showed decreased initial biofilm formation when TCE or CCDE were used, but cell adhesion generally increased when PE was used; this was dependent on conditioning film concentration. Biofilms produced under flow conditions were all reduced by cellular extract conditioning of the surfaces. Multifractal analysis was used to quantitatively analyse the upper percentage coverage of the bacteria and biofilms on the surfaces but more importantly, it was used to quantify the number of cell clusters on the surfaces. Using quantitative descriptors has the potential to help understanding the effect of conditioning films on the adhesion of bacteria and their subsequent biofilm formation.

Abbreviations

BSA	bovine serum albumin
CCDE	cytoplasm with cellular debris
D_q	fractal dimensions
DAPI	4',6-diamidino-2-phenylindole
EPS	extracellular polymeric substances
OD	optical density
PE	periplasmic extract
PPFC	parallel plate flow chamber
SD	standard deviation
SEM	scanning electron microscopy
TCE	total cell extract
ΔG	free energy of interaction
γ^+	electron acceptor parameter

γ^-	electron donor parameter
γ^{AB}	Lewis acid-base component of the surface free energy
γ^{LW}	Lifshitz-van der Waals component of the surface free energy
γ^{Tot}	total surface free energy
θ	contact angle
S_a	average surface roughness
S_{pv}	value of the peak to valley surface roughness
S_q	root mean square of surface roughness

Acknowledgments

This work was financially supported by: Project POCI-01-0145-FEDER-006939 (Laboratory for Process Engineering, Environment, Biotechnology and Energy - LEPABE funded by FEDER funds through COMPETE2020 - Programa Operacional Competitividade e Internacionalização (POCI) - and by national funds through FCT - Fundação para a Ciência e a Tecnologia. L.C. Gomes acknowledges the receipt of a PhD grant from FCT (SFRH/BD/80400/2011).

References

Bernbom, N., Licht, T.R., Saadbye, P., Vogensen, F.K., Norrung, B., 2006. *Lactobacillus plantarum* inhibits growth of *Listeria monocytogenes* in an in vitro continuous flow gut model, but promotes invasion of *L. monocytogenes* in the gut of gnotobiotic rats. Int. J. Food Microbiol. 108, 10-14.

Bernbom, N., Ng, Y.Y., Jorgensen, R.L., Arpanaei, A., Meyer, R.L., Kingshott, P., Vejborg, R.M., Klemm, P., Gram, L., 2009. Adhesion of food-borne bacteria to stainless steel is reduced by food conditioning films. J. Appl. Microbiol. 106, 1268-1279.

Bernbom, N., Vogel, B.F., Gram, L., 2011. *Listeria monocytogenes* survival of UV-C radiation is enhanced by presence of sodium chloride, organic food material and by bacterial biofilm formation. Int. J. Food Microbiol. 147, 69-73.

Bruinsma, G.M., van der Mei, H.C., Busscher, H.J., 2001. Bacterial adhesion to surface hydrophilic and hydrophobic contact lenses. Biomaterials 22, 3217-3224.

Chapman, R.G., Ostuni, E., Liang, M.N., Meluleni, G., Kim, E., Yan, L., Pier, G., Warren, H.S., Whitesides, G.M., 2001. Polymeric thin films that resist the adsorption of proteins and the adhesion of bacteria. Langmuir 17, 1225-1233.

Dat, N.M., Manh, L.D., Hamanaka, D., Hung, D.V., Tanaka, F., Uchino, T., 2014. Surface conditioning of stainless steel coupons with skim milk, buttermilk, and butter serum solutions and its effect on bacterial adherence. Food Control 42, 94-100.

Di Ciccio, P., Vergara, A., Festino, A.R., Paludi, D., Zanardi, E., Ghidini, S., Ianieri, A., 2015. Biofilm formation by *Staphylococcus aureus* on food contact surfaces: relationship with temperature and cell surface hydrophobicity. Food Control 50, 930-936.

Falconer, K., 2013. Fractals - A Very Short Introduction, first ed. Oxford University Press, Oxford.

Falconer, K., 2014. Fractal Geometry: Mathematical Foundations and Applications, third ed. John Wiley and Sons, Chichester.

Garrido, K.D., Palacios, R.J.S., Lee, C., Kang, S., 2014. Impact of conditioning film on the initial adhesion of *E. coli* on polysulfone ultrafiltration membrane. J. Ind. Eng. Chem. 20, 1438-1443.

Goldberger, A.L., Amaral, L.A., Hausdorff, J.M., Ivanov, P., Peng, C.K., Stanley, H.E., 2002. Fractal dynamics in physiology: alterations with disease and aging. Proc. Natl. Acad. Sci. USA 1, 2466-2472.

Gomes, L.C., Moreira, J.M.R., Miranda, J.M., Simões, M., Melo, L.F., Mergulhão, F.J.,

2013. Macroscale *versus* microscale methods for physiological analysis of biofilms formed in 96-well microtiter plates. J. Microbiol. Methods 95, 342-349.

Gomes, L.C., Moreira, J.M.R., Teodósio, J.S., Araújo, J.D.P., Miranda, J.M., Simões, M., Melo, L.F., Mergulhão, F.J., 2014. 96-well microtiter plates for biofouling simulation in biomedical settings. Biofouling 30, 1-12.

Halsey, T.C., Jensen, M.H., Kadanoff, L.P., Procacia, I.I., Shraiman, B.I., 1986. Fractal measures and their singularities: the characterization of strange sets. Phys. Rev. A 33, 1141-1151.

Hamadi, F., Asserne, F., Elabed, S., Bensouda, S., Mabrouki, M., Latrache, H., 2014. Adhesion of *Staphylococcus aureus* on stainless steel treated with three types of milk. Food Control 38, 104-108.

Hammond, A., Dertien, J., Colmer-Hamood, J.A., Griswold, J.A., Hamood, A.N., 2010. Serum inhibits *P. aeruginosa* biofilm formation on plastic surfaces and intravenous catheters. J. Surg. Res. 159, 735-746.

He, X., Liu, Y., Huang, J., Chen, X., Ren, K., Li, H., 2015. Adsorption of alginate and albumin on aluminum coatings inhibits adhesion of *Escherichia coli a*nd enhances the anti-corrosion performances of the coatings. Appl. Surf. Sci. 332, 89-96.

Hentschel, H.G.E., Procaccia, I., 1983. The infinite number of generalized dimensions of fractals and strange attractors. Physica D. 8, 435-444.

Hwang, G., Kang, S., El-Din, M.G., Liu, Y., 2012. Impact of conditioning films on the initial adhesion of *Burkholderia cepacia*. Colloids Surf., B. 91, 181-188.

Hwang, G., Liang, J., Kang, S., Tong, M., Liu, Y., 2013. The role of conditioning film formation in *Pseudomonas aeruginosa* PAO1 adhesion to inert surfaces in aquatic environments. Biochem. Eng. J. 76, 90-98.

Ivanov, P.C., Amaral, L.A.N., Goldberger, A.L., Havlin, S., Rosenblum, M.G., Struzik, Z.R.,

Stanley, H.E., 1999. Multifractality in human heartbeat dynamics. Nature 399, 461-465.

Janczuk, B., Chibowski, E., Bruque, J.M., Kerkeb, M.L., Caballero, F.G., 1993. On the consistency of surface free energy components as calculated from contact angles of different liquids: an application to the cholesterol surface. J. Colloid Interface Sci. 159, 421-428.

Kropp, J., Block, A., von Bloh, W., Klenke, T., Schellnhuber, H.J., 1997. Multifractal characterization of microbially induced magnesian calcite formation in Recent tidal flat sediments. Sediment. Geol. 109, 37-51.

Li, H., Giger, M.L., Olopade, O.I., Lan, L., 2007. Fractal analysis of mammographic parenchymal patterns in breast cancer risk assessment. Acad. Radiol. 14, 513-521.

Lorite, G.S., Rodrigues, C.M., de Souza, A.A., Kranz, C., Mizaikoff, B., Cotta, M.A., 2011. The role of conditioning film formation and surface chemical changes on *Xylella fastidiosa* adhesion and biofilm evolution. J. Colloid Interf. Sci. 359, 289-295.

Lynch, S., 2014. Dynamical Systems with Applications Using MATLAB®, second ed. Springer, Basel.

Mahalik, N.P., Nambiar, A.N., 2010. Trends in food packaging and manufacturing systems and technology. Trends Food Sci. Tech. 21, 117-128.

Martinez, L.R., Casadevall, A., 2007. *Cryptococcus neoformans* biofilm formation depends on surface support and carbon source and reduces fungal cell susceptibility to heat, cold, and UV light. Appl. Environ. Microbiol. 73, 4592-4601.

Merghni, A., Kammoun, D., Hentati, H., Janel, S., Popoff, M., Lafont, F., Aouni, M., Mastouri, M., 2016. Quantification of *Staphylococcus aureus* adhesion forces on various dental restorative materials using atomic force microscopy. Appl. Surf. Sci. 379, 323-330.

Mergulhão, F.J., Monteiro, G.A., Cabral, J.M.S., Taipa, M.A., 2001. A quantitative ELISA for monitoring the secretion of ZZ-fusion proteins using SpA domain as immunodetection reporter system. Mol. Biotechnol. 19, 239-244.

Mills, S.L., Lees, G.C., Liauw, C.M., Lynch, S., 2004. An improved method for the dispersion assessment of flame retardant filler/polymer systems based on the multifractal analysis of SEM images. Macromol. Mater. Eng. 289, 864-871.

Mills, S.L., Lees, G.C., Liauw, C.M., Rothon, R.N., Lynch, S., 2005. Prediction of mechanical properties following the dispersion assessment of flame retardant filler/polymer composites based on the multifractal analysis of SEM images. J. Macromol. Sci. B 44, 1137-1151.

Moore, G., Blair, I.S., McDowell, D.A., 2007. Recovery and transfer of *Salmonella typhimurium* from four different domestic food contact surfaces. J. Food Prot. 70, 2273-2280.

Moreira, J.M.R., Araújo, J.D.P., Miranda, J.M., Simões, M., Melo, L.F., Mergulhão, F.J., 2014. The effects of surface properties on *Escherichia coli* adhesion are modulated by shear stress. Colloids Surf., B 123, 1-7.

Moreira, J.M.R., Gomes, L.C., Araújo, J.D.P., Miranda, J.M., Simões, M., Melo, L.F., Mergulhão, F.J., 2013. The effect of glucose concentration and shaking conditions on *Escherichia coli* biofilm formation in microtiter plates. Chem. Eng. Sci. 94, 192-199.

Moreira, J.M.R., Gomes, L.C., Simões, M., Melo, L.F., Mergulhão, F.J., 2015a. The impact of material properties, nutrient load and shear stress on biofouling in food industries. Food Bioprod. Process. 95, 228–236.

Moreira, J.M.R., Ponmozhi, J., Campos, J.B.L.M., Miranda, J.M., Mergulhão, F.J., 2015b. Micro and macro flow systems to study *Escherichia coli* adhesion to biomedical materials. Chem. Eng. Sci. 126, 440-445.

Oliver, D.B., 1987. Periplasm and protein secretion, in: Neidhardt, F.C., Ingraham, J.L., Low, K.B., Magasanik, B., Schaechter, M., Umbarger, H.E. (Eds.), *Escherichia coli* and *Salmonella typhimurium*: Cellular and Molecular Biology. American Society for Microbiology, Washington DC, pp. 56-69.

Parry, B.R., Surovtsev, I.V., Cabeen, M.T., O'Hern, C.S., Dufresne, E.R., Jacobs-Wagner, C., 2014. The bacterial cytoplasm has glass-like properties and is fluidized by metabolic activity. Cell 156, 183-194.

Pratt-Terpstra, I.H., Weerkamp, A.H., Busscher, H.J., 1987. Adhesion of oral *Streptococci* from a flowing suspension to uncoated and albumin-coated surfaces. J. Gen. Microbiol. 133, 3199-3206.

Ras, M., Lefebvre, D., Derlon, N., Paul, E., Girbal-Neuhauser, E., 2011. Extracellular polymeric substances diversity of biofilms grown under contrasted environmental conditions. Water Res. 45, 1529-1538.

Renner, L.D., Weibel, D.B., 2011. Physicochemical regulation of biofilm formation. MRS Bull. 36, 347-355.

Ribeiro, M.C., da Silva Fernandes, M., Yoshiteru Kuaye, A., Jimenez-Flores, R., Gigante, M., 2017. Preconditioning of the stainless steel surface affects the adhesion of *Bacillus cereus spores*. Int. Dairy J. 66, 108-114.

Robitaille, G., Choinière, S., Ells, T., Deschènes, L., Mafu, A.A., 2014. Attachment of *Listeria innocua* to polystyrene: effects of ionic strength and conditioning films from culture media and milk proteins. J. Food Prot. 77, 427-434.

Teodósio, J.S., Simões, M., Melo, L.F., Mergulhão, F.J., 2011. Flow cell hydrodynamics and their effects on *E. coli* biofilm formation under different nutrient conditions and turbulent flow. Biofouling 27, 1-11.

van Oss, C., 1994. Interfacial Forces in Aqueous Media. Marcel Dekker Inc., New York.

Whitehead, K.A., Benson, P., Smith, L.A., Verran, J., 2009a. The use of physicochemical methods to detect organic food soils on stainless steel surfaces. Biofouling 25, 749-756.

Whitehead, K.A., Benson, P., Verran, J., 2009b. Differential fluorescent staining of *Listeria monocytogenes* and a whey food soil for quantitative analysis of surface hygiene. Int. J. Food

Microbiol. 135, 75-80.

Whitehead, K.A., Smith, L.A., Verran, J., 2010. The detection and influence of food soils on microorganisms on stainless steel using scanning electron microscopy and epifluorescence microscopy. Int. J. Food Microbiol. 141, Supplement, S125-S133.

Whitehead, K.A., Verran, J., 2006. The effect of surface topography on the retention of microorganisms. Food Bioprod. Process. 84, 253-259.

Whitehead, K.A., Verran, J., 2007. The effect of surface properties and application method on the retention of *Pseudomonas aeruginosa* on uncoated and titanium-coated stainless steel. Int. Biodeterior. Biodegradation 60, 74-80.

Whitehead, K.A., Verran, J., 2015. Formation, architecture and functionality of microbial biofilms in the food industry. Curr. Opin. Food Sci. 2, 84-91.

Wickens, D., Lynch, S., West, G., Kelly, P., Verran, J., Whitehead, K.A., 2014. Quantifying the pattern of microbial cell dispersion, density and clustering on surfaces of differing chemistries and topographies using multifractal analysis. J. Microbiol. Methods 104, 101-108.

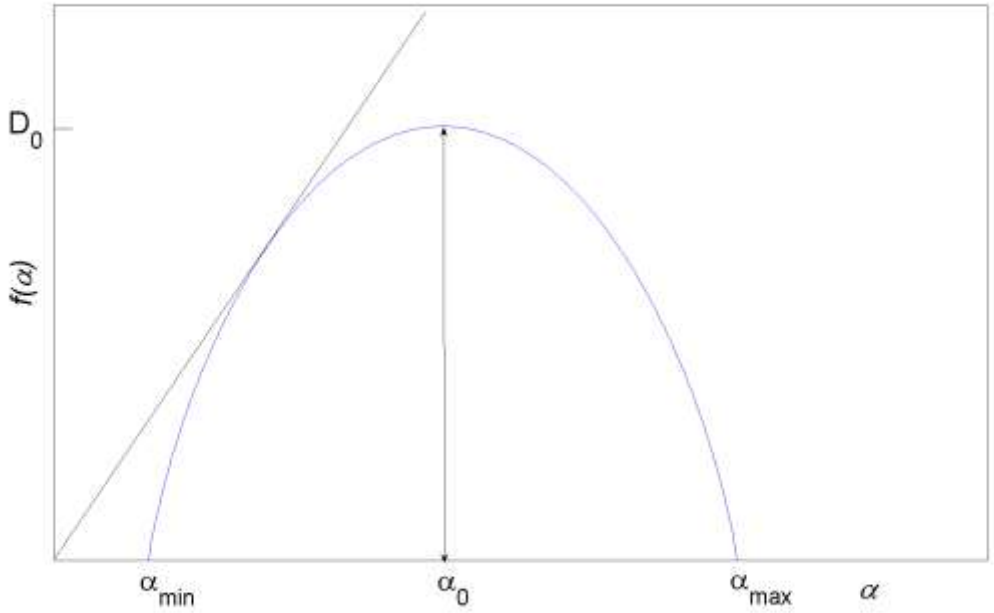

Fig. 1 - A typical $f(\alpha)$ multifractal spectrum with typical denotations of $\alpha_{min,}$ α_0 and α_{max}.

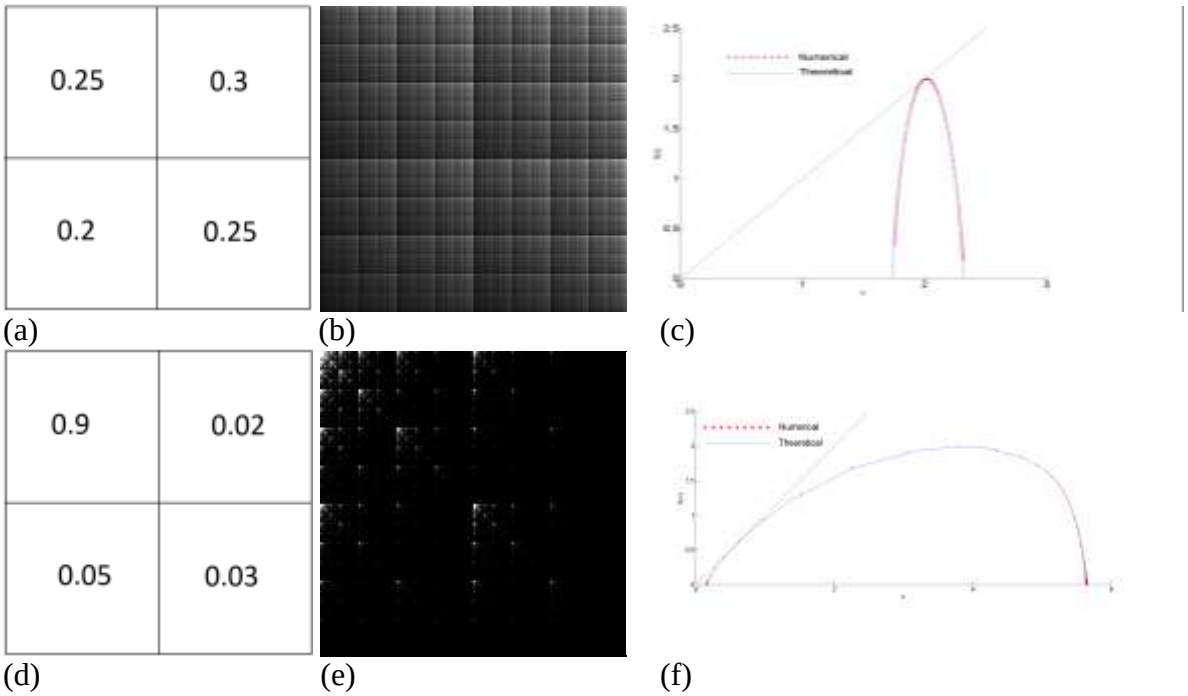

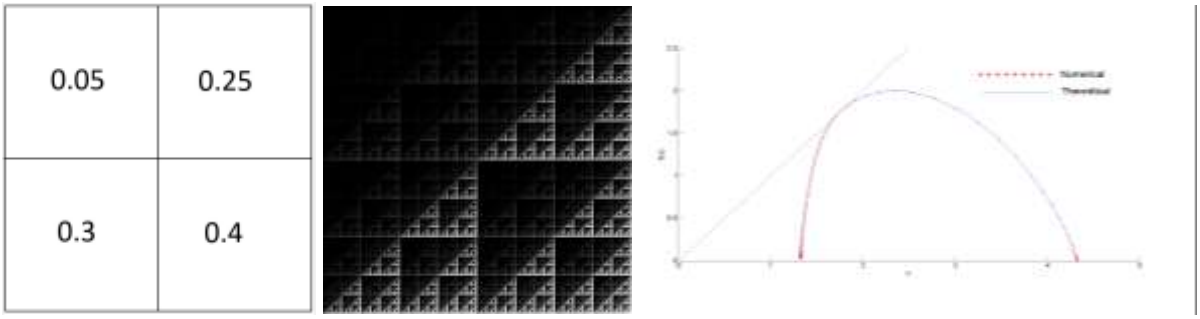

(h) (i) (j)

Fig. 2 - Theoretical and numerical generated $f(\alpha)$ curves for varying motifs and related images: (a) a motif with similar values for all quarters; (b) the grey-scale image for motif (a); (c) near symmetrical $f(\alpha)$ curve indicating low clustering and a homogeneous distribution; (d) a motif with one quarter much higher than the other three; (e) the grey-scale image for motif (d); (f) a left-skewed $f(\alpha)$ curve with $\Delta_{\alpha_{AS}} > 1$, indicating high clustering of dark pixels (gaps in practice); (g) a motif with one quarter much lower than the others; (b) the grey-scale image for motif (g); (i) a right-skewed $f(\alpha)$ curve with $\Delta_{\alpha_{AS}} < 1$, indicating high clustering of lighter pixels (cells in practice).

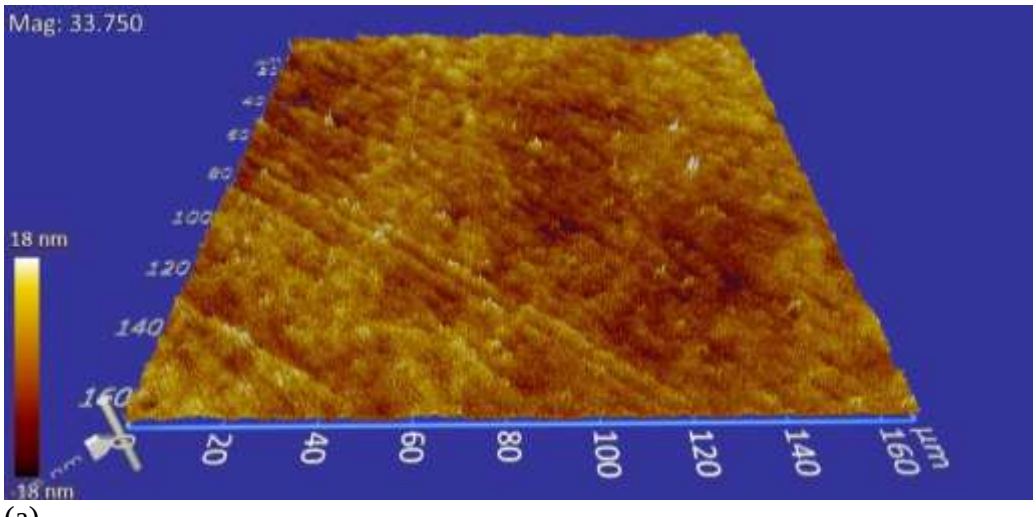

(a)

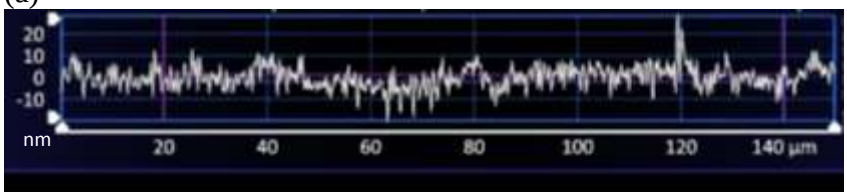

(b)

Fig. 3 – Image (a) and line profile (b) demonstrating the surface topography of the polystyrene substrata.

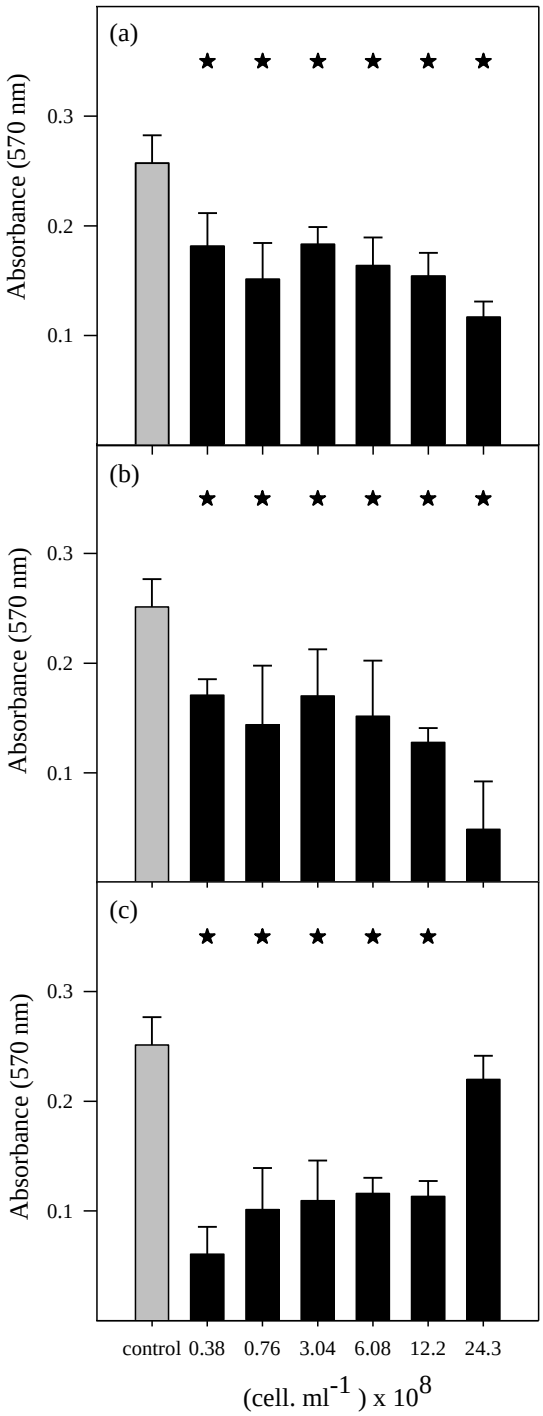

Fig. 4 - *E. coli* biofilm formation (absorbance at 570 nm) after 24 h in 96-well microtiter

plates preconditioned with (a) TCE, (b) CCDE and (c) PE at different concentrations. Biofilm formed on unconditioned surface was used as control. The means ± SD for three independent experiments are presented. Statistical analysis for a confidence level greater than 95% ($P < 0.05$) is marked with an asterisk (*).

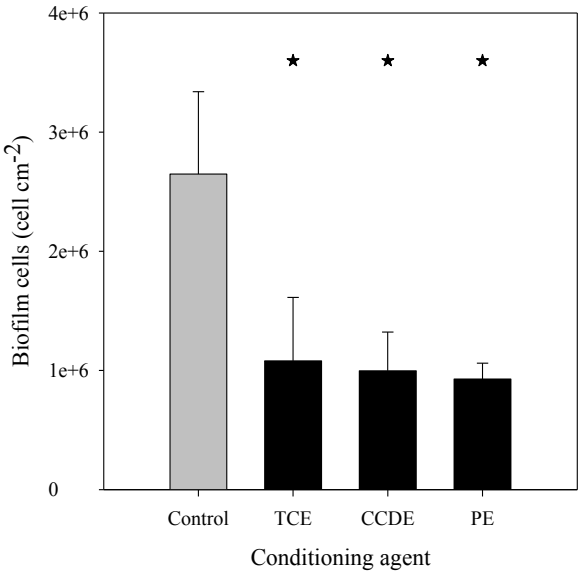

Fig. 5 - Number of biofilm cells per cm^2 after 24 h on preconditioned polystyrene with TCE (corresponding to a cellular concentration of 24.3×10^8 cell ml^{-1}), CCDE (corresponding to a cellular concentration of 24.3×10^8 cell ml^{-1}) and PE (corresponding to a cellular concentration of 0.38×10^8 cell ml^{-1}) in the PPFC. Biofilm formed on unconditioned surface was used as control. The means ± SD for three independent experiments are presented. Statistical analysis for a confidence level greater than 95% ($P < 0.05$) is marked with an asterisk (*).

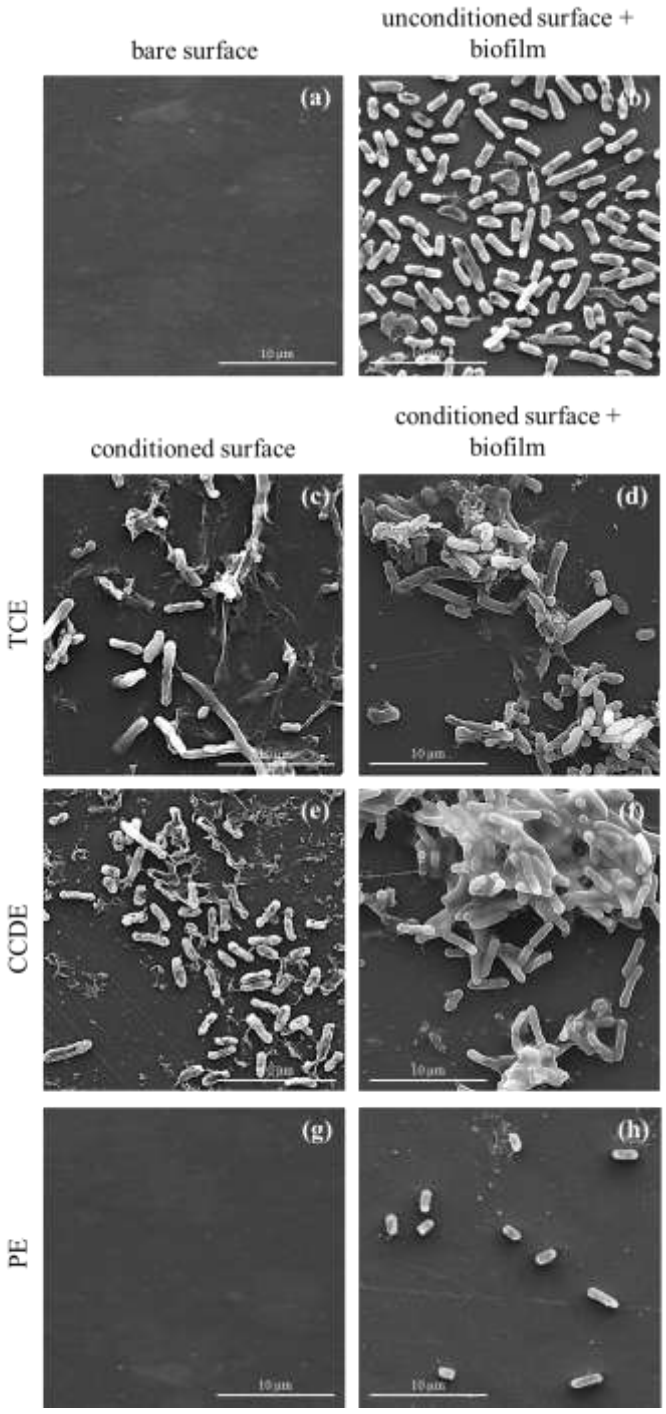

Fig. 6 - Scanning electron micrographs of (a) bare polystyrene surface, (b) unconditioned surface covered by 24 h biofilm, (c, e and g) conditioned surfaces and (d, f and h) conditioned surfaces covered by 24 h biofilms. Micrographs (c) and (d) correspond to TCE, (e) and (f) correspond to CCDE, and (g) and (h) correspond to PE (magnification: 10,000×; bars = 10 μm).

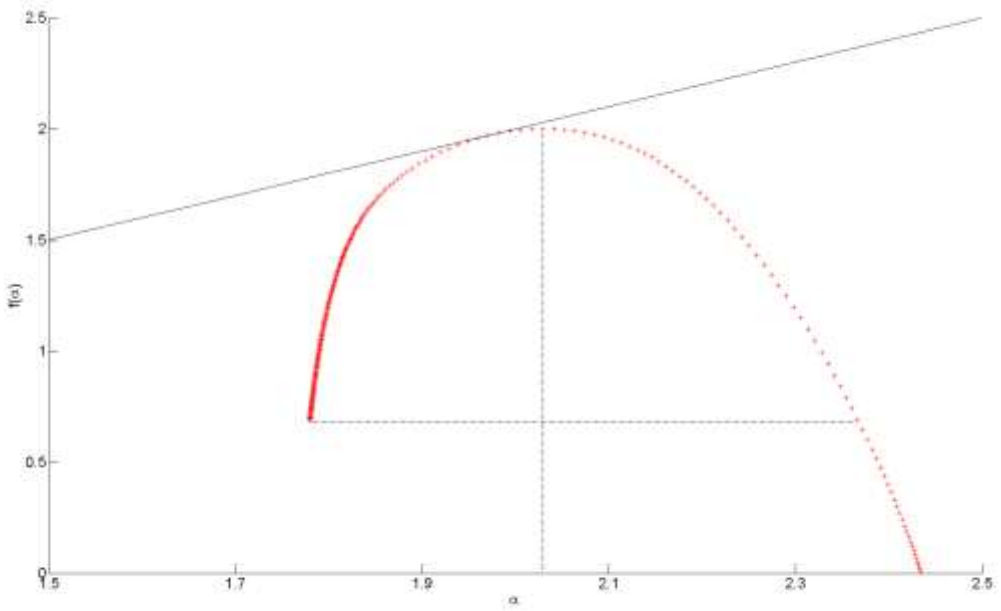

(a)

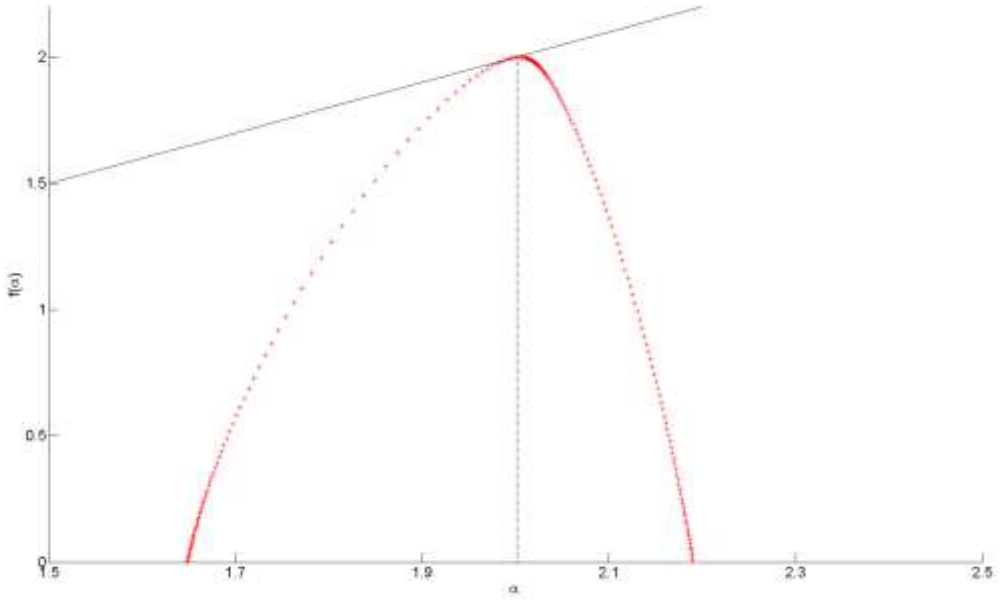

(b)

Fig. 7 - $f(\alpha)$ curves demonstrating the level of skewness ($\Delta_{\alpha_{AS}}$). (a) A right-skewed $f(\alpha)$ curve ($\Delta_{\alpha_{AS}}$≈0.74) corresponding to Fig. 6f and demonstrating cell clustering; (b) a left-skewed $f(\alpha)$ curve ($\Delta_{\alpha_{AS}}$≈ 1.84) corresponding to Fig. 6h and demonstrating mainly gaps.

(a) No cells	
 (b)	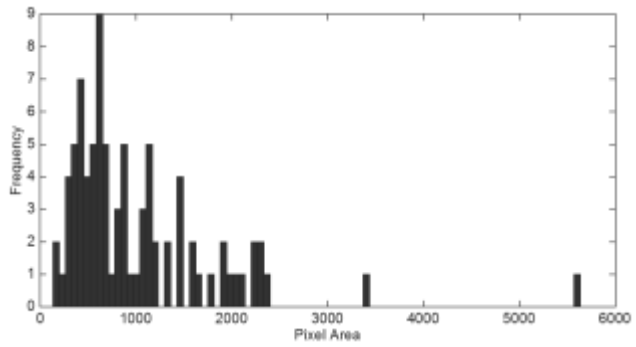
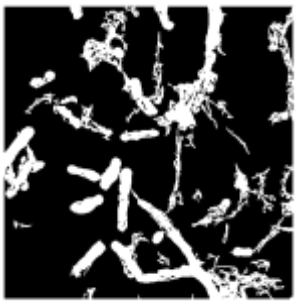 (c)	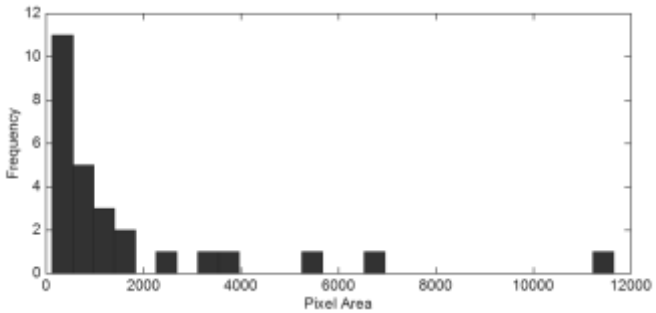
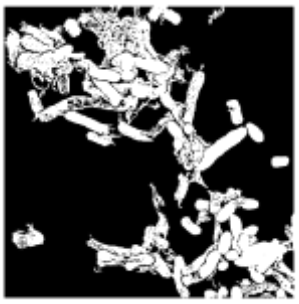 (d)	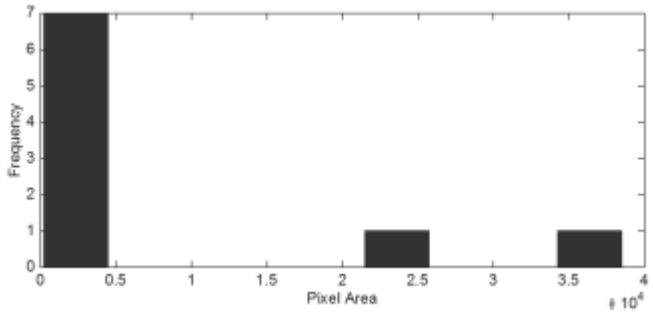
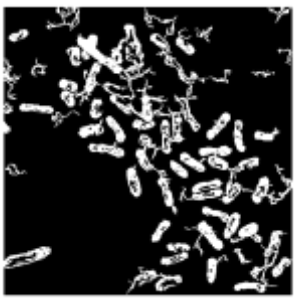 (e)	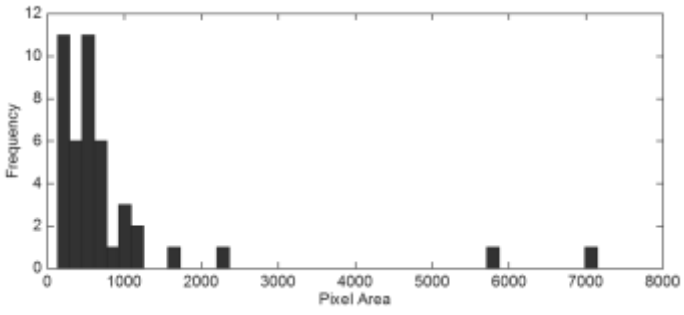

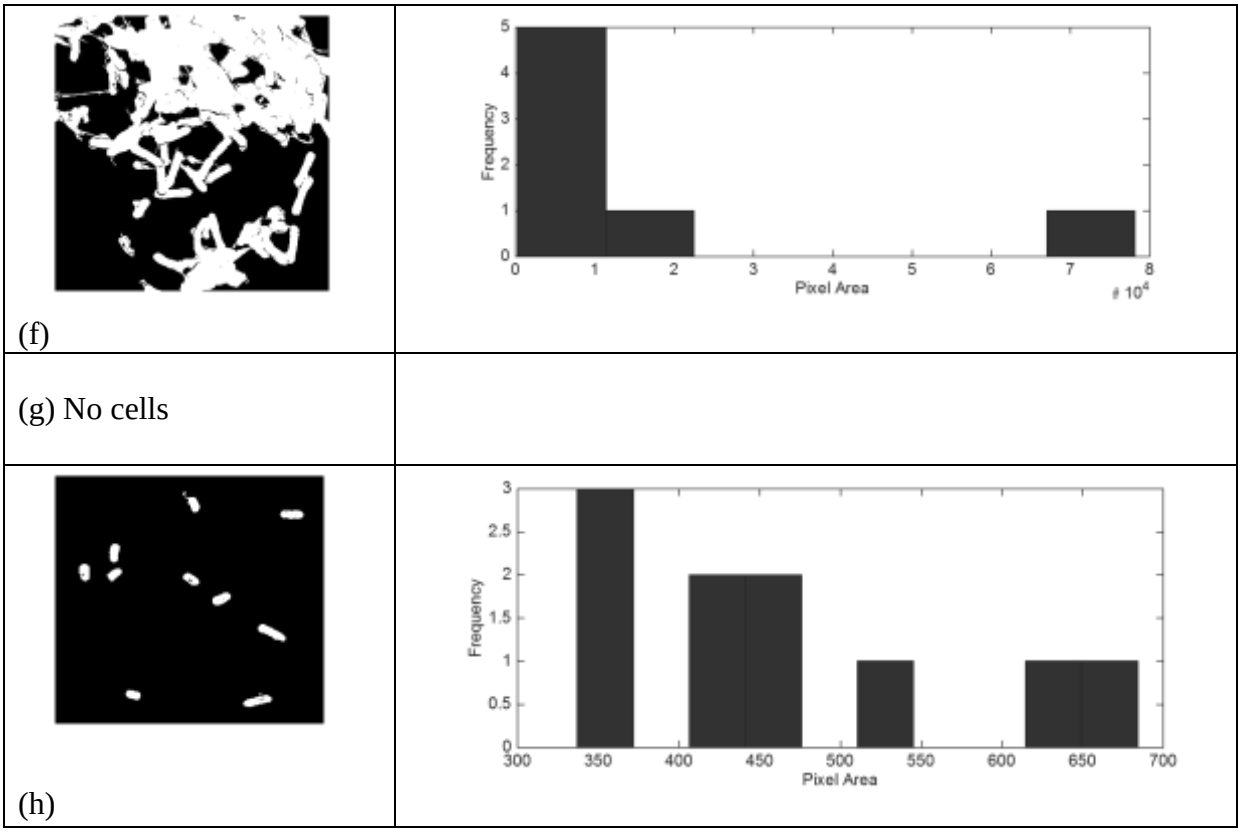

(f)

(g) No cells

(h)

Fig. 8 - Binary images and histograms demonstrating the level of cell clustering across the surfaces: (a) no cells; (b) well distributed cells with lots of coverage (111 objects, percentage coverage = 35.6%, maximum area = 3320 pixels); (c) cells more in clusters (25 objects, percentage coverage = 16.2%, maximum area = 9119 pixels); (d) cells clustered (19 objects, percentage coverage = 28.8%, maximum area = 29953 pixels); (e) well distributed cells (48 objects, percentage coverage = 16.3%, maximum area = 5809 pixels); (f) few cells but clustered (10 objects, percentage coverage = 39.7%, maximum area = 72389 pixels); (g) no cells; (h) few well distributed cells (10 objects, percentage coverage = 2.3%, maximum area = 677 pixels).

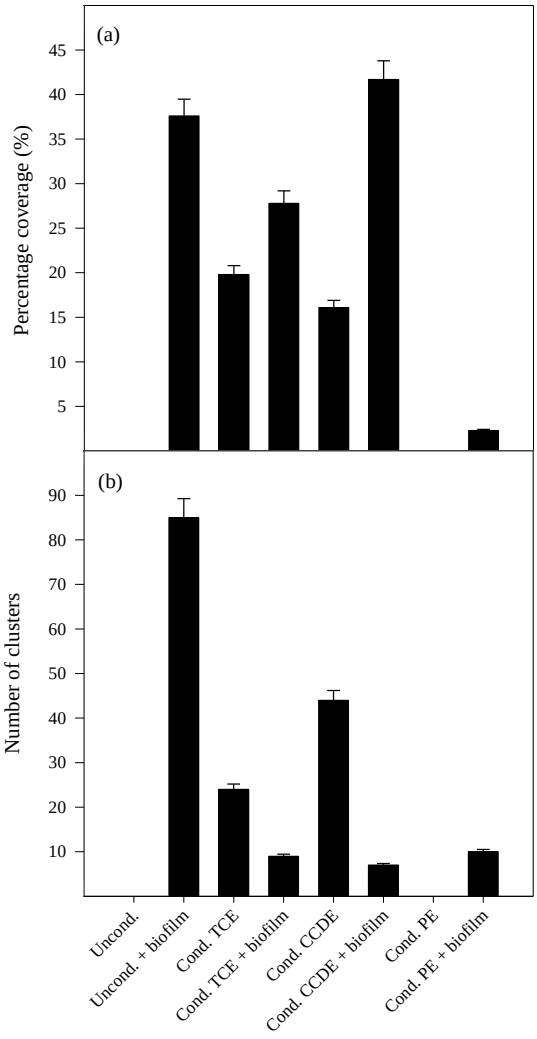

Fig. 9 - (a) Percentage coverage and (b) number of clusters following extrapolation of binary images, $f(\alpha)$ curves and histogram data demonstrating that alongside percentage coverage cell clustering gives further information on the distribution of the cells.

Table 1. Contact angles with water (θ_w), formamide (θ_F) and α-bromonaphthalene (θ_B), hydrophobicity (ΔG) and roughness (S_a, S_q and S_{pv}) of the bare polystyrene and conditioned surfaces. Values are means ± SDs of three independent experiments

	Contact angle (°)				Hydrophobicity (mJ m^{-2})		Roughness (nm)		
	θ_w	θ_F	θ_B		(ΔG)		S_a	S_q	S_{pv}
Bare polystyrene	81.1 ± 0.682	64.3 ± 1.24	24.6 ± 1.11		-50.8		8.01 ± 0.766	12.1 ± 0.731	1082 ± 309
Polystyrene + TCE	69.6 ± 0.984	65.5 ± 1.07	44.7 ± 1.22		-8.79		69.2 ± 25.5	96.0 ± 22.0	2197 ± 695
Polystyrene + CCDE	57.1 ± 0.654	55.4 ± 0.47	69.7 ± 1.70		37.6		69.6 ± 17.2	107 ± 22.7	2600 ± 1302
Polystyrene + PE	77.1 ± 1.93	61.2 ± 2.12	34.2 ± 0.77		-42.1		6.75 ± 0.680	11.0 ± 2.88	1052 ± 349.1